Physical origin of the resonant mode deep inside the stop band of a metallodielectric photonic crystal

Minfeng Chen,[1,2] Shawn-Yu Lin,[2,*] Hung-Chun Chang,[1,3] and Allan S. P. Chang[2]
[1]*Graduate Institute of Photonics and Optoelectronics, National Taiwan University, Taipei, Taiwan, Republic of China*
[2]*Future Chips Constellation & Department of Physics, Applied Physics and Astronomy, Rensselaer Polytechnic Institute, Troy, New York 12180, USA*
[3]*Department of Electrical Engineering and Graduate Institute of Communication Engineering, National Taiwan University, Taipei, Taiwan 106-17, Republic of China*
(Received 4 November 2007; revised manuscript received 16 July 2008; published 8 August 2008)

The first band of a typical layer-by-layer metallodielectric woodpile structure corresponds to the waveguide cutoff of the rod-to-rod opening. However, a nonlocalized propagating mode beyond waveguide cutoff was previously observed if the metallic gratings are separated by dielectric spacers. We show the physical origin of this mode by studying the electromagnetic fields inside the photonic crystal using the finite-difference time-domain analysis. Our results indicate that it is due to an unusual Fabry-Perot resonance between every other grating layer. Moreover, the polarization dependence of transmission spectrum with odd-number layer is a consequence of the symmetry of the grating structure.

DOI: 10.1103/PhysRevB.78.085110 PACS number(s): 42.25.Bs, 78.20.Bh

Photonic crystals (PhCs) have received great interests in recent years.[1] Several three-dimensional (3D) PhCs that exhibit complete photonic band gaps (PBGs) have been proposed, including Yablonovite (a type of slanted pores),[2] inverted opal,[3] and square spiral.[4] The woodpile PhC (Refs. 5 and 6) also possesses a complete PBG. While a pure dielectric PhC is sufficient to obtain a complete 3D PBG, metallic PhC gives the possibility of opening up a relatively large one. It has been shown that the tungsten woodpile PhC has a large PBG down to infrared wavelengths of around 6 μm with a rod-to-rod opening of 3 μm.[7] This band edge is now known as the result of waveguide cutoff for the metal gratings, which is about twice the opening between metal rods.[8]

However, by using the transfer-matrix method, Sang *et al.*[9] numerically predicted that an additional propagating mode beyond waveguide cutoff arises when the metallic layers in the woodpile are separated from each other by dielectric spacers. Moreover, it was pointed out that the propagating mode splits in energy when the number of layers increases from four to eight.[8] Previously, Chang *et al.*[10] confirmed the existence of this mode experimentally. This mode provides an extra degree of freedom to control the flow of light inside a PBG and may lead to potential applications, e.g., control of spontaneous light emission.

The goal of this paper is to investigate the underlying physics of such an allowed mode with numerical demonstration. Through summing up the phase contribution from various elements inside the structure, our results show that this mode is due to equivalent Fabry-Perot cavity inherently present inside the structure. The intrinsic cavity might play an important role in the designs and applications of woodpile PhCs. For example, this additional propagating mode is flat band[10] thanks to its resonance nature. This can be designed for "slow light," "stopping light," and "field concentration."[11–13] Also due to its polarization dependence for odd layers, it can be designed for polarization switching.

A metallodielectric woodpile PhC is schematically depicted in Fig. 1. Each layer in the PhC is in fact a metallic grating with rectangular metal rods and the inter-rod slits are filled with a dielectric with refractive index n. These layers are stacked along the z axis with a dielectric (same as in inter-rod slits) spacer between adjacent layers and each metallic grating layer is laterally rotated 90° from its immediate grating neighbors. Our conjecture is that an equivalent Fabry-Perot cavity can be formed between every other metallic grating layer in this woodpile structure, which is for light linearly polarized along the corresponding grating lines of these layers and with wavelength sufficiently large as compared to the waveguide cut-off condition of the grating. The resultant Fabry-Perot resonances account for the propagating mode beyond waveguide cutoff observed in Refs. 9 and 10.

In this interpretation, a minimum of three layers of metallic gratings are required in the woodpile structure in order for a cavity to be formed, and it is formed between the top layer (layer 1) and the bottom layer (layer 3). There are thus three

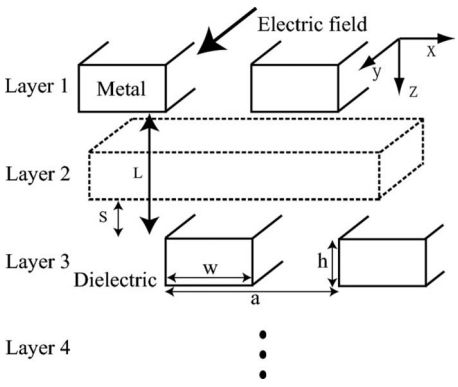

FIG. 1. Configuration of the modified woodpile structure. Each layer is composed of metallic gratings and the layers are stacked along the z axis with a spacer (s) between adjacent layers. The metal rods in odd layers (layer 1, 3, etc.) are oriented along the y axis while those in even layers (layer 2, 4, etc.) are oriented along the x axis.

elements that contribute to the single-pass phase difference in the cavity: the phase due to the reflections at layers 1 and 3, the phase due to the effect of layer 2, and the path-length difference due to optical length of the cavity.

To determine the phase due to layers 1 and 3, we begin with a simple geometry using a two-layer structure, corresponding to the first and third layers in a woodpile structure, with electric field applied parallel to the first layer, as seen in Fig. 1. We perform the simulations using the finite-difference time-domain (FDTD) method[14] with the pitch size $a=300$ nm, the rod width $w=105$ nm, the rod thickness $h=85$ nm, and the spacer $s=85$ nm. For simplicity, our simulation takes the Drude model for gold rods with the plasma frequency $f_p=2172$ THz and the relaxation time $\tau=27.4$ fs.[15] The surrounding refractive index, n, is chosen to be 1.4.

Considering a grating slit (opening between gold rods in a single grating layer), electrodynamic theory tells us that the waveguide cut-off condition of the metal/dielectric/metal slit geometry[16] is $\lambda_{\text{cutoff}}=2(a\text{-}w)\cdot n$ for electric field polarized along the metal/dielectric interface. For wavelengths far above the cut-off wavelength, only evanescent wave is present in the slits. Therefore, very few light tunnels through the one-layer structure for an optically thick metallic film and most of the light is reflected accordingly. A one-layer metallic grating can thus be regarded as a "reflector" for this polarization at long wavelengths. However, a two-layer (or two-reflector) structure can behave differently since two reflectors can in effect form a cavity between them. High transmission occurs when the phase matching condition is fulfilled in the cavity, such that

$$\lambda_{\text{res}}/2 = \frac{L \cdot n}{m}, \tag{1}$$

where L is defined as the distance between the two reflectors and m is a positive integer. For the first-order resonance, $m=1$, the phase difference is $1\cdot\pi$ from one reflector to the other.

Figure 2(a) shows the FDTD-computed transmission spectra of a two-layer structure with various L's. The solid, dashed, and dotted lines correspond to $L=255$, 355, and 455 nm, respectively. The Fabry-Perot resonance is formed in between the two-layer structure, exhibiting resonance transmission peaks with Lorentzian line shape. The waveguide cutoff is around 0.63 μm. Furthermore, the peak wavelength redshifts with increasing L. These evidences are indicative of the Fabry-Perot resonance. The total single-pass phase in the cavity is comprised of two parts: the phase due to L and the phase shift due to each reflector. Since we have assumed the distance, L, in the calculation and there must be π phase shift between two reflectors at resonance, we record the first-order resonant wavelengths due to various L's and calculate the phase contributed from the reflectors at each resonance. This calculated reflector phase contribution as a function of the resonant wavelength is plotted as open circles in Fig. 2(b). We repeat the same procedure with $w=150$ nm and the result is indicated by solid circles in Fig. 2(b). We also plot the phase shifts on flat Au/dielectric interfaces for comparison, as depicted by the solid line in Fig. 2(b). The phase contribution from the reflectors monotonically decreases with wavelength in all three cases. With a narrower slit width, the electromagnetic (EM) wave experiences a larger attenuation in the slit and barely penetrates through the grating layer. As a result, the reflector behaves more like a flat metal plate. We believe this is the reason why solid circles are closer to the solid line in Fig. 2(b). Moreover, Fig. 2(b) implies that at a given wavelength a greater phase shift is contributed by a reflector with larger slit width. To visualize the field penetration, we compute the cavity mode of E_y component in the xz plane with $L=255$ nm at $\lambda_{\text{res}}=1.05$ μm, as displayed in Fig. 2(c). The color denotes the field strength. Red and blue colors correspond to positive and negative field values, respectively. The mode profile indeed shows an exponential decay behavior in the slit, having its maximum value at the center of the cavity.

We next consider the three-layer metallic woodpile, as depicted in Fig. 1(a), by adding an intermediate grating layer between the two reflectors with its grating orientation rotated 90° from that of the reflectors. Note that the EM wave may directly pass through a grating if it is polarized perpendicular to grating lines without suffering a waveguide cutoff. Figure 3(a) shows the 3D FDTD-computed transmission spectra of three-layer woodpiles for two orthogonal linear polarizations. Solid and dashed lines correspond to the polarizations along y (E_y) and x (E_x) axes, respectively. For x polarization, only the second layer acts as a reflector. Hence, no cavity is created, leading to low transmittance throughout the whole wavelength range beyond waveguide cutoff. On the other hand, exactly one cavity is formed between first and third layers for y polarization, resulting in high transmission at resonance with $\lambda_{\text{res}}=1.27$ μm. Compared with the solid line in Fig. 2(a) that shows transmission spectrum for a two-layer structure with the same physical cavity thickness, we notice that λ_{res} is redshifted by 0.22 μm. To analyze how the second layer influences the cavity, we compute the mode profile of E_y component in the yz plane for a single second layer at wavelength of 1.27 μm, as displayed in Fig. 3(b). Observing the light propagation through the grating region, the EM waves couple with the grating by exciting a waveguide mode in the slits. This waveguide mode is known to consist of coupled surface-plasmon polaritons.[17] When reaching the bottom interface of the grating, the EM wave couples out of it and returns to the plane wave. Two significant features associated with the light coupling through the grating are the field enhancement in the slits, shown in Fig. 3(b), and the phase delay. We obtain the phase delay by comparing the phase shifts with and without this grating layer, which gives approximately 0.082π. This phase delay is attributed to the effect of the coupling of light into and out of the grating region.

With the above knowledge, we are equipped to determine the total single-pass phase difference in a three-layer metallodielectric woodpile PhC. Shown in Fig. 3(c) is the configuration of phase contributions in the structure where θ_0 is the phase shift contributed by a reflector and θ_1 is the phase delay caused by the middle grating layer. Phase matching condition demands that

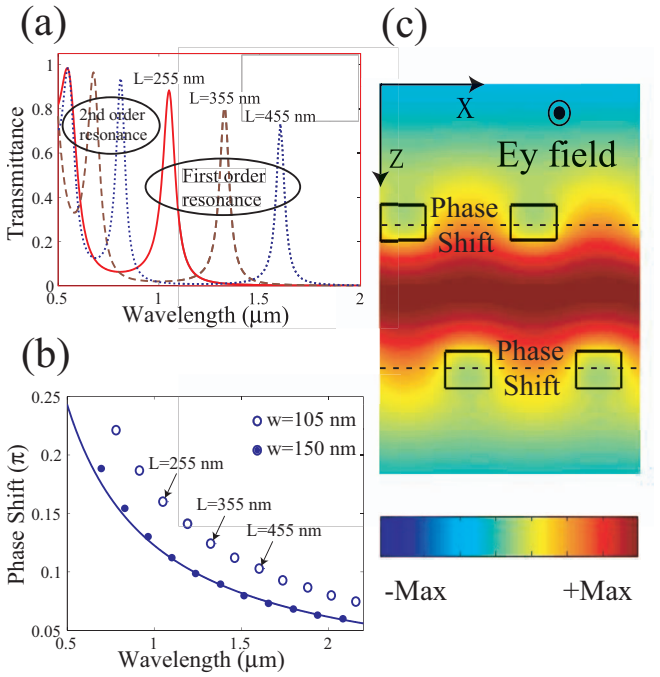

FIG. 2. (Color) (a) The FDTD-computed transmission spectra of a two-layer structure, which contains layers corresponding to first and third layers in a woodpile, with various L's and the electric field is linearly polarized along the y axis. The solid, dashed, and dotted lines correspond to $L=255$, 355, and 455 nm, respectively. The Fabry-Perot resonance is formed in between the two-layer structure, exhibiting resonance transmission peaks. (b) The FDTD-deduced phase shift at the interface between a single grating layer and the dielectric ($n=1.4$). The open and solid circles indicate $w=105$ and 150 nm, respectively. The solid line is an analytical phase shift calculated from the flat interface between gold and dielectric. (c) The E_y cavity mode at resonance of $\lambda_{res}=1.05$ μm with $L=255$ nm. The dark red represents the strongest field value. The electric field penetrates into the slits with an exponential decay behavior, which contributes to additional phase decay.

$$2\theta_0 + \theta_1 + \frac{L \cdot n}{\lambda_{res}/2}\pi = m\pi, \tag{2}$$

where θ_0 can be obtained from Fig. 2(b), given the resonant wavelength $\lambda_{res}=1.27$ μm, which is estimated to be 0.135π, and $\theta_1 \approx 0.082\pi$ as determined above. By putting in all the values, the left side of Eq. (2) yields 0.914π, which is slightly below 1π. All the phases are calculated by two-dimensional (2D) FDTD method where Maxwell's equations are decomposed into two modes. In calculating the phase due to reflectors, only E_y, H_x, and H_z components are required while in calculating the phase from the middle layer, it demands that the other components: H_y, E_x, and E_z, be taken into account. However, in the actual three-layer crystals, the structure is a 3D one, which means those modes are coupled to each other. This may explain the difference between the calculated 0.914π and the 1π by the resonance condition.

In general, the polarization dependence of transmission spectra with odd-number crystal layer can be understood by examining the symmetry of the grating structure. Additionally, the cavity resonance is used to produce the sharp,

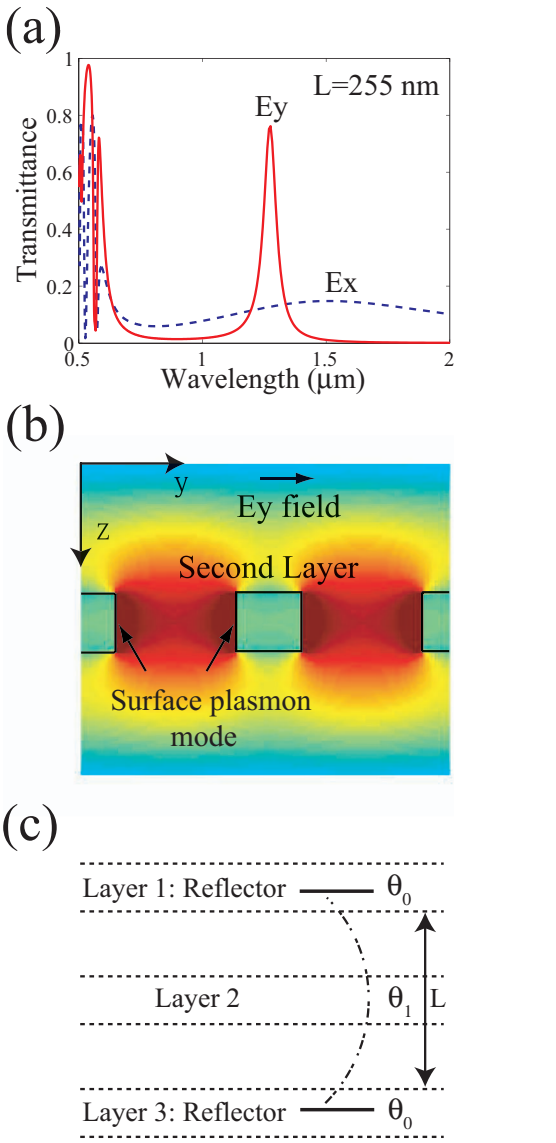

FIG. 3. (Color) (a) The 3D FDTD-computed three-layer (first, second, and third layers) woodpile transmission spectra. The solid and dashed lines correspond to the polarizations along the y and x axes, respectively. Contrary to the x polarization where no cavity is established, there is one cavity present for the y polarization. Therefore, one resonance peak is observed in the calculation result. (b) The mode profile of the E_y field in a single second layer. At this polarization, the EM wave can directly pass through the grating through plasmonic excitation. (c) The schematic of phase contribution from each layer.

polarization-dependent transmission peaks. With more PhC layers, a cascade of cavities can be possibly created and thus split the transmission peak due to the coupling between those identical cavities. In the following section we analyze the exact geometry of a five-layer PhC as our fabricated sample given in Ref. 10, which is made up of gold rods surrounded by the dielectric material known as hydrogen silsesquioxane (HSQ) (Ref. 18) on top of a Si substrate (the corresponding refractive index n of HSQ is 1.4). The different polarizations in Fig. 4 are distinguished by the same line styles as in Fig. 3(a). For x polarization, second and fourth layers form re-

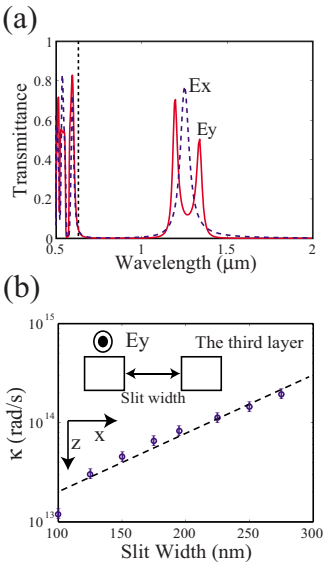

FIG. 4. (Color online) (a) The 3D FDTD-computed spectra of the five-layer woodpile structure. The solid and dashed lines represent the respective same polarizations as shown in Fig. 3(a). For the *y* polarization, two cavities are established, which lead to two transmission peaks. One cavity is formed between the first and third layers, and the other one is between the third and fifth layers. For the *x* polarization, one cavity is present between the second and fourth layers, which results in only one transmission peak. (b) The FDTD-computed coupling coefficient as a function of the slit width. A logarithmic (base 10) scale is used for the *y* axis. The straight dashed line is a guide to eye. The data show exponential growth of coupling strength as the slit width increases.

flectors. Thus there is one transmission peak observed in the spectrum due to one cavity being established, as shown in Fig. 4(a). As for *y* polarization, the first, third, and fifth layers play the role of reflectors, resulting in two cavities. One is between first and third layers, and the other is between third and fifth layers. Those two cavities are identical. Coupling of cavity modes may cause the splitting of the transmission peak, described by the coupling-mode theory:[19] $\omega_{\pm} = \omega_{\text{res}} \pm \kappa$, where ω_{res} is the angular frequency of the uncoupled resonant state, κ is the coupling coefficient, and ω_+ and ω_- are the angular frequencies of the two split states. In our case, the third layer serves as coupling. Both of the cavity modes possess exponential decay at the slit of the third layer, indicative of exponential overlapping for the coupling of modes. We manipulate the coupling strength by varying the slit widths. Shown in Fig. 4(b) is the FDTD-computed coupling coefficient, $\kappa=(\omega_+-\omega_-)/2$, as a function of the slit width of the third layer. A logarithmic (base 10) scale is used for the *y* axis. The straight dashed line is a guide to the eye. The data shows exponential growth of the coupling strength as the slit width increases. This is consistent with our explanation.

It is remarkable that the cavities are established only along the *z* direction. This propagating mode has a Bloch form in the *xy* plane, i.e., it is nonlocalized. It is known that a Fabry-Perot cavity will blueshift at oblique incident angles. Blueshifting of the propagating mode with oblique incidence was indeed observed in Ref. 10. Those evidences further support our interpretation.

In summary, we have investigated the physical origin of the propagating mode in a metallodielectric woodpile PhC by means of the FDTD modeling. It is a direct result of an equivalent Fabry-Perot cavity. Our explanations are consistent with both numerical results and experimental data reported in Ref. 10.

S.Y.L. would like to acknowledge the financial support of AFOSR under Grant No. FA95500610431.

*Author to whom correspondence should be addressed. sylin@rpi.edu

[1] J. D. Joannopoulos, R. D. Meade, and J. N. Winn, *Photonic Crystals* (Princeton University Press, New Jersey, 1995).
[2] E. Yablonovitch, T. J. Gmitter, and K. M. Leung, Phys. Rev. Lett. **67**, 2295 (1991).
[3] K. Busch and S. John, Phys. Rev. E **58**, 3896 (1998).
[4] O. Toader and S. John, Science **292**, 1133 (2001).
[5] K. M. Ho, C. T. Chan, C. M. Soukoulis, and M. Sigalas, Solid State Commun. **89**, 413 (1994).
[6] S. Y. Lin, J. G. Fleming, D. L. Hetherington, B. K. Smith, R. Biswas, K. M. Ho, M. M. Sigalas, W. Zubrzycki, S. R. Kurtz, and J. Bur, Nature (London) **394**, 251 (1998).
[7] J. G. Fleming, S. Y. Lin, I. El-Kady, R. Biswas, and K. M. Ho, Nature (London) **417**, 52 (2002).
[8] Z. Y. Li, I. El-Kady, K. M. Ho, S. Y. Lin, and J. G. Fleming, J. Appl. Phys. **93**, 38 (2003).
[9] H. Y. Sang, Z. Y. Li, and B. Y. Gu, Phys. Rev. E **70**, 066611 (2004).
[10] A. S. P. Chang, Y. S. Kim, M. Chen, Z. P. Yang, J. A. Bur, S. Y. Lin, and K. M. Ho, Opt. Express **15**, 8428 (2007).
[11] M. F. Yanik, W. Suh, Z. Wang, and S. Fan, Phys. Rev. Lett. **93**, 233903 (2004).
[12] M. F. Yanik and S. Fan, Phys. Rev. A **71**, 013803 (2005).
[13] M. F. Yanik and S. Fan, Stud. Appl. Math. **115**, 233 (2005).
[14] A. Taflove and S. C. Hagness, *Computational Electrodynamics: The Finite-Differece Time-Domain Method* (Artech House, Boston, London, 2005).
[15] M. Fox, *Optical Properties of Solids* (Oxford University Press, New York, 2006).
[16] S. Ramo, J. R. Whinnery, and T. V. Duzer, *Fields and Waves in Communication Electronics* (Wiley, New York, 1994).
[17] S. Collin, F. Pardo, R. Teissier, and J.-L. Pelouard, Phys. Rev. B **63**, 033107 (2001).
[18] M. J. Loboda, C. M. Grove, and R. F. Schneider, J. Electrochem. Soc. **145**, 2861 (1998).
[19] H. A. Haus, *Wave and Fields in Optoelectronics* (Prentice-Hall, Englewood Cliffs, NJ, 1984).